Sensors & Diagnostics

PAPER

View Article Online
View Journal | View Issue

Cite this: *Sens. Diagn.*, 2025, **4**, 995

Use of cobalt(II) and chromium(III) metal-based Schiff base complexes for the preparation of potentiometric sensors to determine bromide at ultra-low concentrations

Mohsin Ali,[ac] Kousar Jahan,[b] Jitendra Singh,*[c] Ratnesh Kumar Singh,[d] Sudhir Kumar Shoora,[e] Xu Feng[f] and Yanfeng Yue *[b]

Received 2nd June 2025,
Accepted 17th July 2025

DOI: 10.1039/d5sd00088b

rsc.li/sensors

Co(II) and Cr(III) salicylidene Schiff base-based complexes as novel ionophores were evaluated for the fabrication of bromide-selective electrodes. By incorporating a cation excluder along with various plasticizers (dibutyl phthalate, dioctyl phthalate, 1-chloronapthalene), optimized sensors (CoC7 and CrC7) exhibiting near-Nernstian slopes being 59.4 ± 0.07 and 59.2 ± 0.04 mV decade^{-1}, with a broad linear range (1×10^{-2} to 6.0×10^{-7} and 1×10^{-2} to 8.7×10^{-7} mol L^{-1}), with low detection limits ($5.5 \pm 0.13 \times 10^{-7}$ and $6.5 \pm 0.07 \times 10^{-7}$ mol L^{-1}) respectively, were successfully designed. Selectivity coefficient values of order 10^{-1} or less indicate that the proposed electrodes have superior selectivity for bromide ions over various interfering anions. The developed bromide electrodes demonstrated robust performance within a pH range of 4.0 to 9.0, as well as showing a sufficient shelf life (4 and 5 weeks) with up to 20% (v/v) non-aqueous tolerance and quick response times (12 and 16 s). These electrodes also served as indicator electrodes in the potentiometric titration of bromide ions against $AgNO_3$ and were used in the determination of bromide ion concentration in water samples.

1. Introduction

Bromide (Br^-) is commonly found in both treated and untreated water sources across the world, especially in groundwater. Chlorination or ozonation disinfection methods are extensively employed in drinking water source treatment to eliminate pathogens. However, at low concentrations, these disinfection processes can lead to the formation of various chlorinated and brominated disinfection by-products (DBPs), which cause significant risks to human health. Among these, bromate (BrO_3^-) stands out as particularly concerning. It is generated from bromide as a precursor and has been recognized by the "International Agency for Research on Cancer (IARC)" as a probable human carcinogen.[1–6] Since bromide is a precursor to bromate, its abundance in water sources has a considerable impact on the quality of drinking water. The low amount of bromide ions in the water supplies and drinking water, however, makes their estimation difficult and necessitates the use of sensitive, rapid, and effective instrumental analysis. Many techniques are available for determining the concentration of bromide ions in various substances such as milk, food items, water, wine, and urine. Over the years, numerous analytical techniques have been developed for this purpose, each with its advantages and limitations. These techniques include ion chromatography (IC),[7] ion-pair reversed phase liquid chromatography,[8] high-performance liquid chromatography (HPLC),[9] gas chromatography-mass spectrometry (GCMS),[6] inductively coupled plasma mass spectrometry (ICP-MS),[10] capillary zone electrophoresis,[11] cyclic voltammetry,[12] and chemiluminescence.[13] However, these established techniques often require cumbersome infrastructure, entail high maintenance costs, and can be time-consuming. Moreover, they may not be suitable for high-throughput analysis of large sample sets. As a result, the focus of researchers in recent times has shifted to developing alternative analytical methods that are reliable, cost-effective, rapid, and convenient for *in situ* sample evaluations, such as potentiometric methods.

[a] *Department of Applied Sciences, Modern Institute of Technology and Research Centre, Alwar 301001, India*
[b] *Department of Chemistry, Delaware State University, Dover, Delaware 19901, USA. E-mail: yyue@desu.edu*
[c] *Department of Chemistry, Hemvati Nandan Bahuguna Garhwal University, Srinagar-247174, India. E-mail: jkfcy13@hnbgu.ac.in*
[d] *Department of Chemistry, Government Engineering College, Bhojpur, 802301, India*
[e] *Ministry of Environment, Forest and Climate Change, Government of India, Indira Paryavaran Bhawan, Jorbagh Road, New Delhi, India*
[f] *Surface Analysis Facility, University of Delaware, Newark, DE 19716, USA*

Ion-selective electrodes (ISEs) have emerged as promising tools for ion determination due to their simplicity, portability, and low cost. These electrodes exploit the selective interaction between the target ion and a specific sensing element, allowing for direct measurement without extensive sample preparation or sophisticated instrumentation.[14] Fig. 1 illustrates the components and the selective mechanism for bromide ion detection using the potentiometric method. In this context, attempts were made to develop new bromide (Br^-) ion-selective PVC membranes with the combination of transition metal complexes. The framework of the ligand and the characteristics of the metal ions in the coordination complex play an important role in affecting the Br^- ion selectivity of these electrodes. Given the significance of the determination of Br^- ions, many bromide ion-selective polymeric membrane electrodes have been studied, using different ionophores such as metal complexes HgS/Hg_2Br_2,[15] chalcogenide glassy–crystalline $AgBr\text{-}Ag_2S\text{-}As_2S_3$,[16] 14-phenyldibenzo[*a*,*j*]xanthene,[17] bis(4-hydroxyphenyl)-1,4-diaza-1,3-butadiene mercury(II) complex,[18] iron(III)-salen,[19] *meso*-tetraphenylporphyrin manganese(III) chloride complex and 4,5-dimethyl-3,6-dioctyloxy-*o*-phenylene-bis(mercury trifluoroacetate),[20] mercury(II) complex of a pyridine,[21] graphene oxide–aluminium fumarate metal–organic framework (BGO/AlFu MOF),[22] Pt(II) 5,10,15,20-tetra(4-methoxy-phenyl)-porphyrin(PtTMeOPP),[23] 1,3-dihexadecylimidazolium bromide,[24] and an azapyrylium ion derivative.[25] Isildak *et al.* have used a cobyrinic acid derivative macrocyclic molecule as an ionophore for selective detection of Br^- ions with concentration ranges of 1×10^{-2}–6.0×10^{-7} and 1.0×10^{-1}–1.0×10^{-4} mol L^{-1} and with detection limits of 5.5×10^{-7} and 2.2×10^{-5} mol L^{-1}.[26] While the Br^- ion sensors that were previously reported had strong sensitivity and selectivity towards bromide, many of them were limited by non-Nernstian slope, poor detection limit, and short working concentration range. In the context of existing bromide sensors, there is an urgent need to develop a robust bromide-selective sensor with enhanced potentiometric characteristics for the detection of low bromide concentrations. In this work, Co(II) and Cr(III) salicylidene Schiff base complexes were investigated as ionophores for Br^- ion detection in aqueous media based on a potentiometric method. Interestingly, due to the high stability of the Co(II) and Cr(III) complexes and specific interactions among the metal center and different anions, an improved potentiometric performance for bromide ion detection in terms of high sensitivity, wide linear range, lower detection limit, and high stability in a wide pH range was recorded. Meanwhile, both cobalt and chromium complexes often have flexible coordination numbers and geometries, which can be customized to fit the size and charge of Br^- ions. This flexibility can improve the binding efficiency and stability of halides. Additionally, the facile synthesis methodology and low cost of all precursors make these complexes excellent alternatives to expensive commercial bromide exchangers. The advancement made here will benefit future sensor development to detect other anions, such as environmentally important nutrients including NO_3^- and HPO_4^{2-}. The components and the selective mechanism for bromide ion detection using the potentiometric method are illustrated in Fig. 1. In this context, attempts were made to develop new bromide (Br^-) ion-selective PVC membranes with different combinations of these transition metal complexes. The framework of the ligand and the characteristics of the metal ions in the coordination complex play an important role in affecting the Br^- ion selectivity of these electrodes.

2. Experimental section

2.1. Materials

All analytical grade reagents, including cetyltrimethylammonium bromide (CTAB), dioctyl phathalate (DOP), dibutyl phthalate (DBP), chloronaphthalene (CN), *o*-nitrophenyl octyl ether (NPOE),

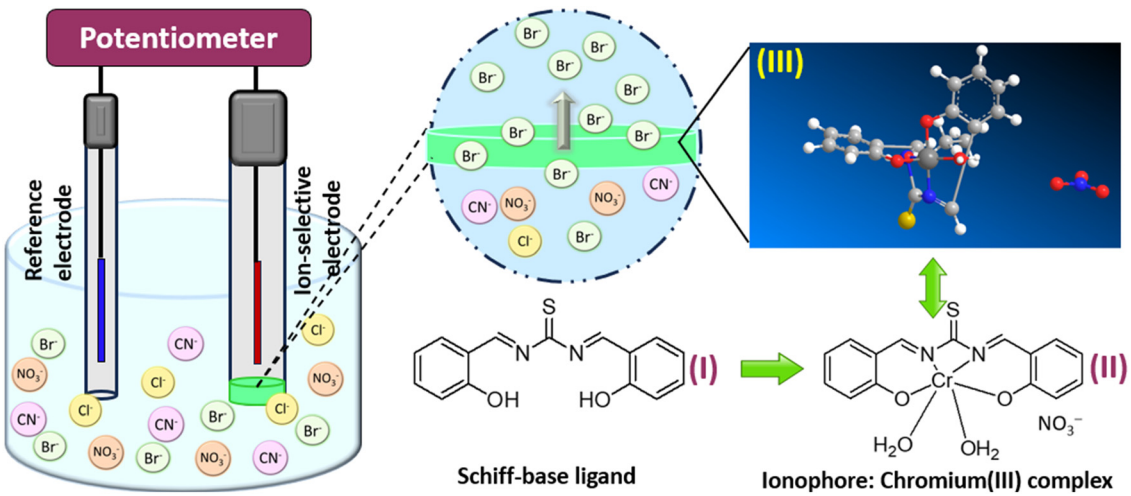

Fig. 1 The components and selective mechanism for bromide ions by using a potentiometric method, with the Cr(III) salicylidene Schiff base complex as an ionophore. Inset: CrC and salicylidene Schiff base prepared in one-pot preparation (I), coordination environment of Cr(III) in the complex CrC, and simulated configuration of the CrC coordination complex.

tri-*n*-butyl phosphate (TBP), tetrahydrofuran (THF), hydrochloric acid, sodium hydroxide, salicylaldehyde, thiourea, cobaltous nitrate, chromium nitrate, polyvinyl chloride (PVC) and sodium bromide were purchased from Hi Media (Mumbai MH, India). Stock solutions (0.1 M) of metal salts were prepared in double distilled water and used to make dilute solutions of required concentrations.

2.2. Synthesis of ionophores

The ionophores Co(II) and Cr(III) salicylidene Schiff base complexes (CoC) and (CrC) were synthesized and characterized by the reported procedure with a slight modification.[27] Salicylaldehyde (10 mmol, 1.22 g) was added to a 20 mL homogeneous ethanolic solution of cobalt(II) and chromium(III) nitrate (5 mmol), taken in a 100 mL round bottom flask and the pH of the solution was maintained between 6 and 8 using a liquid ammonia solution. Then, a 10 mL ethanolic solution of thiourea (5 mmol, 0.38 g) was mixed with the above solution and this mixture was continuously refluxed for 8 hours. Upon cooling the reaction mixtures to room temperature, Co(II) and Cr(III) Schiff base complexes were separated as dark brown and dark green precipitates. These precipitates were filtered and washed with cold ethanol and dried in a vacuum desiccator. Co(II) and Cr(III) Schiff base complexes showed the following characteristics: $[C_{15}H_{12}N_2O_3SCo](NO_3)_2$ yield: 75.5%; m.p. 143 °C; and $[C_{15}H_{10}N_2O_2SCr](NO_3)\cdot(H_2O)_{6.7}$ yield: 79.5%; m.p. ~173 °C.

2.3. Preparation of electrodes

PVC membrane electrodes based on CoC and CrC were prepared according to the method described by Craggs.[30] To prepare a uniform mixture, membrane components including ionophores (CoC) and (CrC), cationic additive (CTAB), plasticizers (DBP, CN, DOP, *o*-NPOE, and TBP), and PVC were dissolved in about 5 mL of THF. This concentrated mixture was evenly filled into polyacrylate rings with an internal diameter of 2 cm affixed on a flat glass plate. It was then allowed to evaporate at room temperature (25 ± 2 °C) for 24 h under ambient humidity (40–50%) and the membrane rings were covered, and kept it for a whole day at room temperature to evaporate the solvent. After careful removal of the ring from the plate, a transparent membrane with a thickness of 0.5 mm was obtained. Subsequently, the membrane was affixed to one end of a glass tube using Araldite and sealed with epoxy resin to avoid leakage of the internal solution.

The membranes were allowed to acclimate in a 1.0×10^{-1} mol L^{-1} NaBr solution for four days. Potentials were recorded by varying the concentration of the NaBr test solution within the range of 1.0×10^{-8}–1.0×10^{-1} mol L^{-1}. Each solution was agitated and the potential was recorded once it reached a stable point. The logarithmic function of the Br^- ion activity was then plotted. A saturated calomel electrode (SCE) was used as the reference electrode for the potential measurements, which were performed at 25 ± 0.1 °C using an Orion 4-star pH metre with the following cell assembly:

Hg/Hg_2Cl_2 |KCl(satd)| 0.1 M NaBr ||PVC membrane|| test solution |Hg/Hg_2Cl_2| KCl(satd).

The activities of Br^- ions were calculated according to the following modified Debye–Huckel approximation (eqn (1)):

$$\log Y = -0.511Z^2\left(\frac{\mu^{1/2}}{1+1.5\mu\frac{1}{2}} - 0.2\mu\right) \quad (1)$$

where Y is the activity coefficient, Z represents the charge on the ion and μ shows the ionic strength.

2.4. Apparatus

Potentiometric experiments were carried out using an ESICO INTERNATIONAL Digital potentiometer Model-118 and the proposed electrode in combination with a double junction Ag/AgCl reference electrode. The pH was obtained using a digital pH meter [ESICO INTERNATIONAL digital pH meter Model-101].

Results and discussion

The ionophores of Co(II) and Cr(III) salicylidene Schiff base complexes (CoC) and (CrC) were synthesized using a facile one-pot method by refluxing the metal nitrate, thiourea, and salicylaldehyde in ethanol according to the reported procedure.[27] Fig. 1 presents the Schiff base ligand (inset I) and one of its corresponding chromium complexes as a representative example (insets II and III). The structure and chemical functionality of the complexes were characterized by ATR-FTIR spectroscopy, X-ray diffraction, X-ray photoelectron spectroscopy, and CHN analysis. The FTIR analysis revealed a characteristic band at 1599 cm^{-1} in the Schiff base ligand, attributed to the stretching vibration of the C=N bond. This indicates successful condensation between the amine group of thiourea and the aldehyde group of salicylaldehyde, resulting in the formation of the Schiff base ligand. In the Co(II) complex, the band appeared slightly shifted to a higher wavenumber at 1625 cm^{-1} and for the Cr(III) complex, this band appeared slightly shifted to a lower wavenumber at 1591 cm^{-1}, suggesting the coordination of azomethine nitrogen with Co and Cr atoms (Fig. S1). The ligand and metal complexes Co(II) and Cr(III) display sharp crystalline peaks in their XRD spectra (Fig. S2), indicating their crystalline nature. Furthermore, XPS analysis was performed to study the oxidation state of Co and Cr after complexation. The survey scan spectra (Fig. S3A) demonstrated the presence of C, N, O, S, Cr and Co in the CoC and CrC complexes. The high resolution spectra of Co 2p displayed single doublet feature characteristics of Co $2p_{3/2}$ at 781.2 eV and Co $2p_{1/2}$ at 787.1 eV and those of Cr 2p displayed single doublet feature characteristics of Cr $2p_{3/2}$ at 577.2 eV and Cr $2p_{1/2}$ at 587.1 eV, confirming a homogenous Co(II) and Cr(III) oxidation state in the complex.[28] CHN elemental analysis of the Co(II) and Cr(III) complexes compared to theoretical calculations suggested the $[C_{15}H_{10}N_2O_2SCo](NO_3)\cdot(H_2O)_{6.}$ and $[C_{15}H_{10}N_2O_2SCr](NO_3)\cdot(H_2O)_{6.7}$ structures for the CoC; Cr(II) and CrC; Cr(III) salicylidene Schiff base complexes (SI; CHN analysis results). Based on the above characterization data, CoC and CrC were

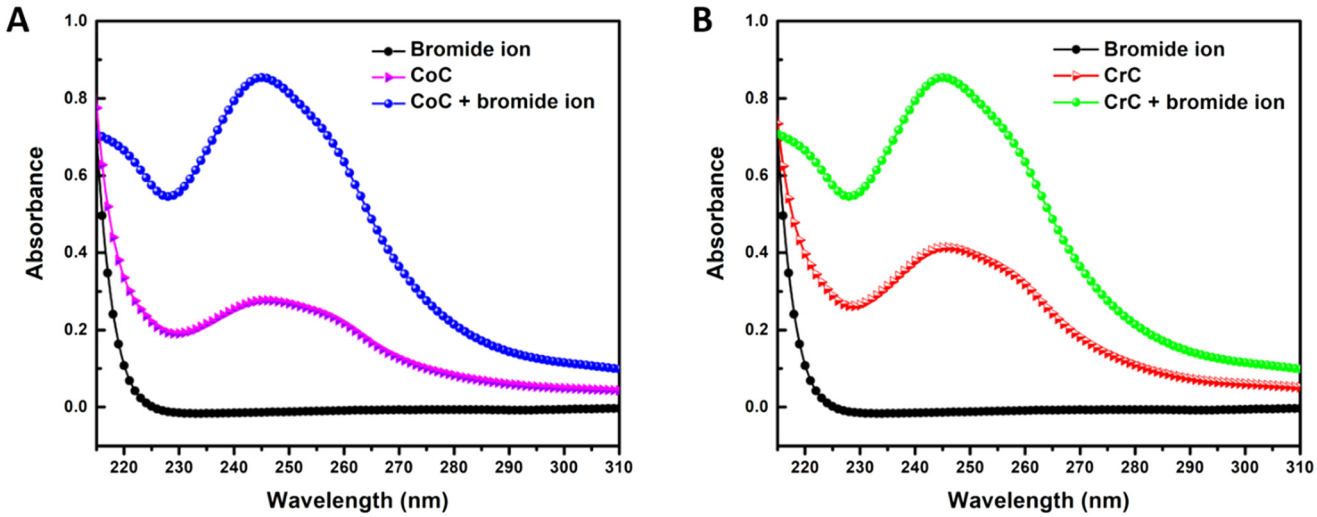

Fig. 2 The absorption spectra of (A) CoC and (B) CrC with bromide ion (NaBr 1.0×10^{-3} mol L^{-1}) solution in MeOH.

confirmed as mononuclear complexes with a Co(II) and Cr(III) to ligand ratio of 1 : 1 (Fig. 1, inset II).

Further, UV-visible (UV-vis) spectroscopy is employed to analyze the interaction between CoC and CrC ionophores and bromide ions due to its capability to detect molecular interactions based on changes in absorbance. UV-vis absorption spectra of CoC and CrC were recorded, using an equimolar quantity of NaBr solution each having a 1.0×10^{-3} mol L^{-1} concentration in methanol. UV-vis spectra, as shown in Fig. 2(A and B), can discern the interlinkage between the metal chelates and bromide ions. The considerable changes in the absorbance of CoC at 245 nm and CrC at 246 and 255 nm were noted in the absorption spectra with an equimolar amount of bromide ion solution.[29] Here, the results strongly imply that ionophores form 1 : 1 complexes with the bromide ion. On the other hand, there were negligible changes in the UV-vis spectra of CoC and CrC ionophores when recorded in the presence of other anions. The perceived spectral shifts, coupled with the significant increase in absorbance peaks in the CoC and CrC spectra following the contact with the bromide ion-containing solution, indicate the favorable coordination of the bromide ion with the ionophore. The change in the UV-vis spectra indicates the interaction between the ionophores and bromide ions.

To understand the coordination behavior of both CoC and CrC with different anions, a conductometric titration method was carried out. Conductometric study was performed by titrating 20 mL 1.0×10^{-4} mol L^{-1} of anion solution against 1.0×10^{-2} mol L^{-1} solution of CoC and CrC. The conductance (S cm^{-1}) of the solution was precisely noted for each addition of ionophores. The results showed that among several anions studied, the conductance of the Br^- ion solution was greatly affected with the addition of CoC and CrC. The observed variation in the conductance of the Br^- ion solution with the metal complexes is plotted in Fig. 3, which explains that the conductance of the bromide ion solution starts decreasing quickly with the addition of the metal complexes. Once all bromide ions are consumed, no further change in conductance occurs, resulting in the conductometric titration curve reaching a nearly straight line at the end point. An exact stoichiometry ratio of 1 : 1 is indicated for the final product of the reaction at the end of the conductometric titration curve.

One of the most critical parameters that sheds light on an ion electrode's functional selectivity is the ion–ionophore complexation occurring within the membrane. The sandwich membrane method was employed to calculate the formation constants for the 1 : 1 ion–ionophore complex. A concentration-polarized sandwich membrane was formed by fusing together two membrane segments, of which only one contained the ionophore. The formation constants were then calculated by the following eqn (2):[30]

$$\beta_{\mathrm{IL}_n} = \left(L_{\mathrm{T}} - \frac{nR_{\mathrm{T}}}{Z_{\mathrm{I}}}\right)^{-n} \exp\left(\frac{E_{\mathrm{M}} z_{\mathrm{I}} F}{RT}\right) \quad (2)$$

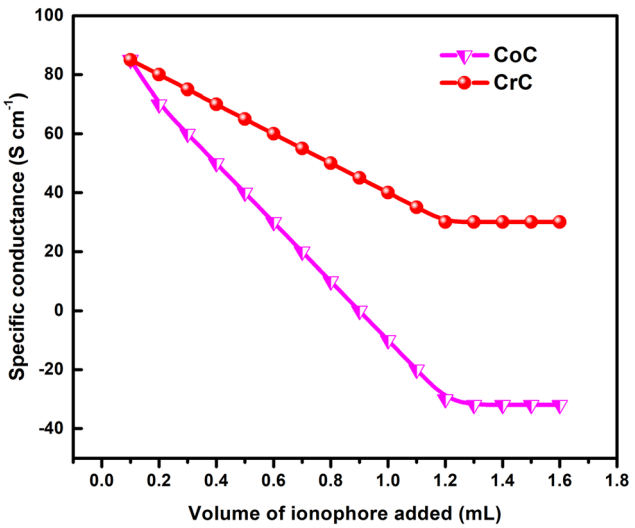

Fig. 3 Variation in the conductance (S cm^{-1}) of bromide ion solutions with CoC and CrC ionophores.

Table 1 Stability constant values of ionophores CoC and CrC with different anions by the sandwich membrane method (n = 3)

Anion (X^{n-})	$(\mathrm{Log}\,\beta_{\mathrm{CoCX}}) \pm \sigma$	$(\mathrm{Log}\,\beta_{\mathrm{CrCX}}) \pm \sigma$
Br^-	7.09 ± 0.16	6.90 ± 0.06
I^-	5.02 ± 0.02	4.91 ± 0.22
Cl^-	4.95 ± 0.35	4.80 ± 0.25
CO_3^{2-}	4.91 ± 0.07	4.75 ± 0.08
SO_4^{2-}	4.83 ± 0.66	4.70 ± 0.55
CN^-	4.57 ± 0.36	4.45 ± 0.32
F^-	4.43 ± 0.26	4.31 ± 0.12
SCN^-	3.72 ± 0.27	3.66 ± 0.10
NO_2^-	3.71 ± 0.16	3.55 ± 0.61
NO_3^-	3.02 ± 0.72	3.04 ± 0.07
Sal^-	2.92 ± 0.26	2.75 ± 0.14

where n represents the ion–ionophore complex stoichiometry, L_T is the total concentration of the ionophore in the membrane segment, R_T is the concentration of lipophilic additives, E_M is the membrane potential and R, T and F are the constants having their usual meaning. z_I is the charge on the ion. The formation constants for different ion–ionophore complexes are given in Table 1. These values revealed that CoC (7.09 ± 0.16) and CrC (6.90 ± 0.06) complexes form the most stable complexes with Br^- ions compared to the other anions. The higher formation constant values with Br^- ions support the notion that CoC and CrC complexes can be looked at as potential ionophores for bromide ion detection and their membranes may serve as bromide selective electrodes.

The compositions of potentiometric membrane electrodes fabricated by incorporating CoC and CrC were optimized by adjusting the amounts of other membrane ingredients.[31] All the electrodes were calibrated in 10^{-1} M NaBr solution before potentiometric studies. The results show the potentiometric characteristics of bromide selective electrodes based on ionophores CoC (CoC**1** to CoC**10**) and CrC (CrC**1** to CrC**10**) which were evaluated as a function of bromide ion concentration in the range of 10^{-8} to 10^{-1} mol L^{-1} (Table 2). The electrodes with 6 mg of CoC and 94 mg PVC (CoC**1**) and 5 mg of CrC and 95 mg of PVC (CrC**1**) exhibited potentiometric characteristics demonstrating sub-Nernstian slopes (36.2 mV per decade for CoC and 38.1 mV per decade for CrC of Br^-), high detection limits (2.5×10^{-4} mol L^{-1} for CoC and 2.0×10^{-4} mol L^{-1} for CrC) with narrow working concentration ranges (5.0×10^{-4}–1.0×10^{-3} mol L^{-1} and 5.5×10^{-4}–1.0×10^{-2} mol L^{-1}). The sensitivity, linearity, and selectivity of given ionophores are significantly influenced by the membrane composition, particularly the type of plasticizer used.[32] Therefore, numerous combinations of membrane constituents (as listed in Tables 2 and 3) were tested to identify the membrane that provides high performance and reproducible results. Subsequently, the membrane electrode with the highest performance was chosen for thorough potentiometric analyses. According to previously published studies, a cation excluder enhances the potentiometric properties of an anion-selective electrode and increases its selectivity.[33] To improve electrode performance,

Table 2 Optimized PVC membrane compositions based on CoC and their potentiometric response as bromide ion selective electrodes

Electrode no.	Membrane ingredients (mg)				Slope (mV per decade of $[Br^-]$)	Linear range (mol L^{-1})	Detection limit (mol L^{-1})
	Ionophore (CoC)	CTAB	Plasticizer	PVC			
CoC1	6	0	0	94	36.2	5.0×10^{-4}–1.0×10^{-3}	2.5×10^{-4}
CoC2	6	3	0	91	45.4	6.9×10^{-5}–1.0×10^{-2}	3.0×10^{-5}
CoC3	6	3	55, DOP	36	51.7	7.1×10^{-6}–1.0×10^{-2}	3.4×10^{-6}
CoC4	6	3	55, NPOE	36	62.4	7.3×10^{-6}–1.0×10^{-2}	3.7×10^{-6}
CoC5	6	3	55, CN	36	63.0	5.3×10^{-6}–1.0×10^{-2}	2.5×10^{-6}
CoC6	6	3	55, TBP	36	56.8	1.5×10^{-6}–1.0×10^{-2}	9.2×10^{-6}
CoC7	6	3	55, DBP	36	59.4	6.0×10^{-7}–1.0×10^{-2}	5.5×10^{-7}
CoC8	5	3	55, DBP	37	57.9	5.7×10^{-6}–1.0×10^{-2}	3.6×10^{-6}
CoC9	7	3	55, DBP	35	59.1	6.2×10^{-6}–1.0×10^{-2}	5.6×10^{-6}
CoC10	6	2	55, DBP	37	57.6	3.7×10^{-6}–1.0×10^{-2}	1.8×10^{-6}

Table 3 Optimized PVC membrane compositions based on CrC and their potentiometric response as bromide ion selective electrodes

Electrode no.	Membrane ingredients (mg)				Slope (mV per decade of $[Br^-]$)	Linear range (mol L^{-1})	Detection limit (mol L^{-1})
	Ionophore (CrC)	CTAB	Plasticizer	PVC			
CrC1	5	0	0	95	38.1	5.5×10^{-4} –1.0×10^{-2}	2.0×10^{-4}
CrC2	5	3	0	92	47.2	5.0×10^{-5}–1.0×10^{-2}	2.5×10^{-5}
CrC3	5	3	55, CN	37	66.5	7.5×10^{-6}–1.0×10^{-2}	3.9×10^{-6}
CrC4	5	3	55, NPOE	37	61.1	4.3×10^{-6}–1.0×10^{-2}	2.6×10^{-6}
CrC5	5	3	55, TBP	37	53.3	1.5×10^{-6}–1.0×10^{-2}	1.1×10^{-6}
CrC6	5	3	55, DOP	37	58.0	5.9×10^{-6}–1.0×10^{-2}	2.1×10^{-6}
CrC7	5	3	55, DBP	37	59.2	8.7×10^{-7}–1.0×10^{-2}	6.5×10^{-7}
CrC8	4	3	55, DBP	38	51.4	4.3×10^{-6}–1.0×10^{-2}	3.6×10^{-6}
CrC9	3	3	55, DBP	39	56.8	9.0×10^{-5}–1.0×10^{-2}	7.0×10^{-5}
CrC10	5	4	55, DBP	36	55.4	4.1×10^{-6}–1.0×10^{-2}	2.2×10^{-6}

a cation exchanger (CTAB) was mixed with the membrane composition. Potential studies given in Tables 2 and 3 revealed that the electrodes (CoC2 and CrC2) having 3 mg CTAB exhibited some improvement in the slope, detection limit and working concentration range.

It was further seen from Table 2 that the membranes of CoC with different types of plasticizers *viz.*, CN, NPOE, TBP, DOP, and DBP (electrode no. CoC3–CoC7) performed better than the membrane without a plasticizer showcasing wider working concentration ranges and improved slopes. DBP plasticized membrane electrode CoC7 showed the best performance among all the plasticized membranes, exhibited the widest working concentration range of 6.0×10^{-7}–1.0×10^{-2} mol L^{-1} with a Nernstian slope of 59.4 mV per decade of [Br^-] and a low detection limit of 5.5×10^{-7} mol L^{-1}. In Table 3, similar results were also obtained with the membranes of CrC with different types of plasticizers *viz.*, CN, NPOE, TBP, DOP, and DBP (electrode no. CrC3–CrC7), which performed better than the membrane without a plasticizer showcasing wider working concentration ranges and improved slopes. DBP plasticized membrane electrode CrC7 showed the best performance among all the plasticized membranes, exhibited the widest working concentration range of 8.7×10^{-7}–1.0×10^{-2} mol L^{-1} with a Nernstian slope of 59.2 mV per decade of [Br^-] and a low detection limit of 6.5×10^{-7} mol L^{-1}. Due to the very low polarity and great mobility of DBP compared to other plasticizers explored, DBP is supposed to provide sufficient conditions for the integration of Br^- ions into the membrane before coordinating with the metal in complexes.[33]

The effect of varying amounts of ionophores (CoC7, CoC8, and CoC9; CrC7, CrC8, and CrC9) was also studied, and it was observed that reducing the ionophore concentration in the membrane phase significantly changed the potentiometric characteristics of the electrodes (CoC8 and CoC9), and CrC8 and CrC9 did not show improved performance. The potentiometric responses similarly decreased for CoC10 and CrC10 which had an increased concentration of CTAB, leading to increased interference from foreign cations in the solution. This is evident from the performance comparison of all these electrodes shown in Tables 2 and 3, indicating that electrodes CoC7 and CrC7 are the best-performing electrodes, and the optimum composition of CoC7 is determined to be CoC : DBP : CTAB : PVC in a ratio of 6 : 55 : 3 : 36 (mg) and that of CrC7 is determined to be CrC : DBP : CTAB : PVC in a ratio of 5 : 55 : 3 : 37 (mg). The potential responses of the CoC and CrC7 electrodes were evaluated by contentiously changing the internal solution from 1.0×10^{-1} to 1.0×10^{-8} mol L^{-1} and their potentiometric data were observed from their calibration curve. The study found minor differences in the Nernstian slope of the electrodes in dilute solutions (1.0×10^{-3} and 1.0×10^{-4} mol L^{-1}), affecting their operating range and detection limitations. Therefore, the suitable concentration of internal Br^- solution was determined to be 1.0×10^{-2} mol L^{-1} for further studies of CoC7 and CrC7.

The equilibration time of ISEs is an important parameter affecting their performance. For the activation of electrodes, the potential response of the electrodes was measured after soaking them in a 1.0×10^{-2} mol L^{-1} bromide solution for distinct time periods. Stable and reproducible results were obtained after conditioning the electrodes for a period of 12 hours. However, extending the equilibration time beyond 12 hours showed no improvement in the performance of CoC7 and CrC7. The best performing electrodes, CoC7 and CrC7, were used under the above-explained state. The calibration plots of these electrodes shown in Fig. 4 show that they can operate over broad working concentration ranges (6.0×10^{-7}–1.0×10^{-2} mol L^{-1} and 8.7×10^{-7}–1.0×10^{-2} mol L^{-1}) showing Nernstian responses (59.4 and 59.2 mV per decade of [Br^-])

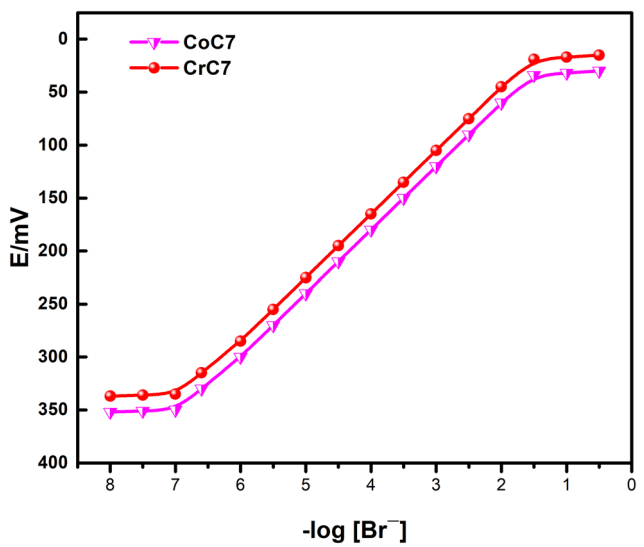

Fig. 4 Calibration curves for the best performing electrodes CoC7 and CrC7.

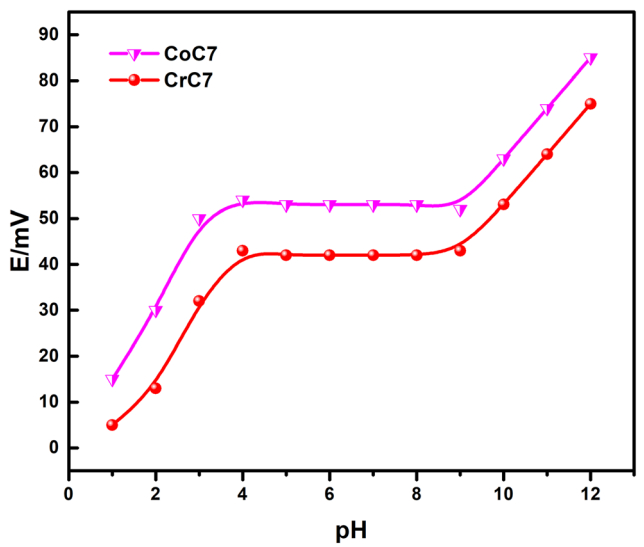

Fig. 5 Effects of pH on the performance of proposed electrode solutions with bromide at a concentration of 1.0×10^{-2} mol L^{-1}.

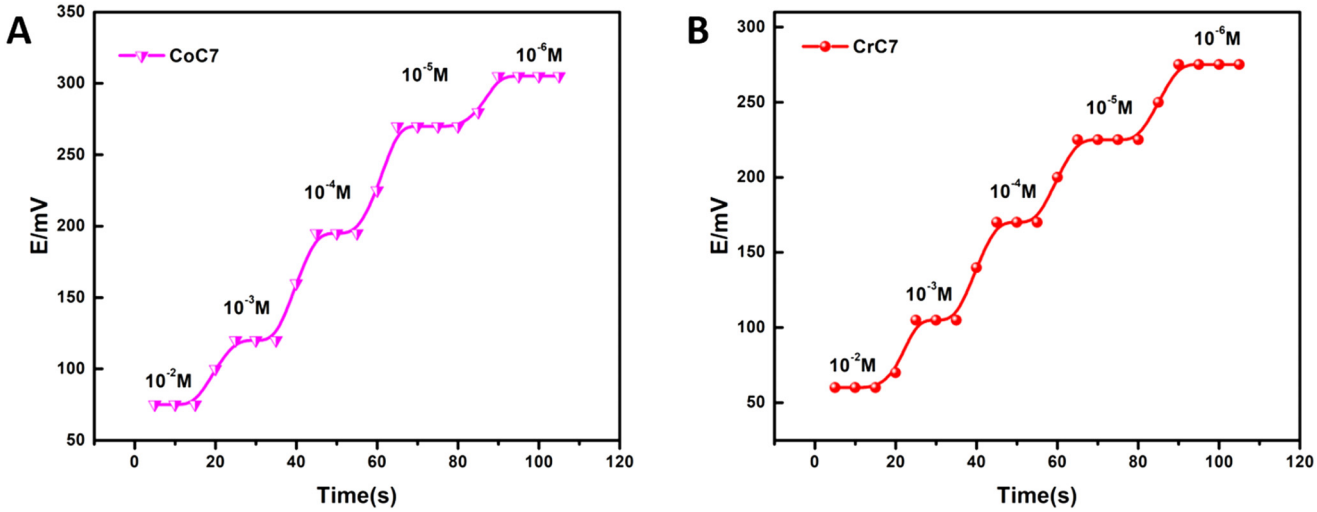

Fig. 6 (A and B) Dynamic response times of CoC7 and CrC7 electrodes.

with lower detection limits of 5.5×10^{-7} and 6.5×10^{-6} mol L^{-1}, respectively.

For the determination of a suitable pH range for the considered electrode, the effect of pH on the performance of CoC7 and CrC7 was assessed in 1.0×10^{-2} M mol L^{-1} bromide ion solution. The pH range between 1.0 and 12.0 was adjusted by the addition of a desired amount of dilute HCl and NaOH solutions. The potential response for this study is shown in Fig. 5, showing that the potentials remained unchanged within the pH range of 4.0 to 9.0, making this working pH range suitable for further studies. The deviations in potentials beyond this pH range may be attributed to the oxidation of bromide in the acidic solution (below pH 4.0) and as a result of hydrolysis (above pH 9.0) of metal complexes. To determine the response time of the suggested electrodes, the concentration of the Br^- solution was sequentially changed from 1.0×10^{-2} mol L^{-1} to 1.0×10^{-6} mol L^{-1}. The potential responses are depicted in Fig. 6(A and B), and the results suggested that the time required for obtaining the stable potential value after immersing the electrodes successively in a series of bromide ion solutions is 12 and 16 seconds for CoC7 and CrC7, respectively. This study indicates rapid exchange kinetics between bromide ions and ionophores at the solution–membrane interface. To examine the reversibility of these electrodes, the process was reversed by measuring the potential from high to low concentrations and the response time of these electrodes remained unchanged. Furthermore, the reproducibility of the electrodes was also checked with a set of three duplicate electrodes of CoC7 and CrC7, and their potentiometric investigations were performed under identical conditions. The results were found to be in good agreement (±0.06 mV), indicating their reliable and reproducible performance.

The lifetime of an ISE is an important feature that describes its active lifespan for accurately estimating primary ions in the test solution. To evaluate the lifetime of the proposed bromide selective electrodes, ee, the proposed electrodes were used daily over a period of 1 hour each day for 2 months (8 weeks). The slopes and detection limits were measured from the derived calibration plots, as shown in Table 4. The experimental results showed that there was no significant change in the potentiometric characteristics of electrodes CoC7 and CrC7 up to 5 weeks. However, the potential responses of these electrodes gradually deteriorated over time, showing sub-Nernstian slopes and elevated detection limits. It is noteworthy that the electrodes were stored in 0.1 M NaBr solution when not in use.

The functions of both CoC7 and CrC7 electrodes were also evaluated in partially non-aqueous solutions as shown in Table 5 with methanol–water, ethanol–water and acetonitrile–water solutions of different concentrations, and calibration curves were recorded. It was observed that that the electrodes could tolerate up to 20% (v/v) non-aqueous content as there was negligible change in their slope and linear working range at this concentration. However, above 20% non-aqueous content, the slope and working range are considerably reduced, which could be due to membrane degradation from leaching of ionophores or other ingredients from the PVC matrix.

Selectivity is a crucial response characteristic of an ion selective electrode; it permits the prediction of how an ISE will perform in the analysis of real-life samples. The IUPAC

Table 4 Lifetime study of the proposed electrodes CoC7 and CrC7

Time (weeks)	Electrode CoC		Electrode CrC	
	Slope (mV)	Detection limit (mol L^{-1})	Slope (mV)	Detection limit (mol L^{-1})
1	59.4 ± 0.2	5.5×10^{-7}	59.2 ± 0.2	6.5×10^{-7}
2	59.4 ± 0.04	5.5×10^{-7}	59.2 ± 0.3	6.5×10^{-7}
3	59.4 ± 0.5	5.8×10^{-7}	59.1 ± 0.4	6.8×10^{-7}
4	59.2 ± 0.3	6.5×10^{-7}	59.1 ± 0.4	6.8×10^{-7}
5	59.1 ± 0.4	4.1×10^{-6}	59.0 ± 0.6	7.5×10^{-7}
6	58.2 ± 0.7	5.5×10^{-6}	58.8 ± 0.7	3.5×10^{-6}
7	57.6 ± 0.8	9.4×10^{-5}	58.2 ± 0.9	4.5×10^{-6}
8	56.9 ± 0.5	1.5×10^{-5}	57.1 ± 0.5	1.7×10^{-5}

Table 5 Performance of the proposed electrodes in partially non-aqueous media

	Electrode CoC7		Electrode CrC7	
Non-aqueous content (%, v/v)	Working concentration range (mol L^{-1})	Slope (mV per decade [Br])	Working concentration range (mol L^{-1})	Slope (mV per decade [Br])
Nil	6.0×10^{-7}–1.0×10^{-2}	59.4	8.7×10^{-7}–1.0×10^{-2}	59.2
Methanol				
10	6.0×10^{-7}–1.0×10^{-2}	59.4	8.7×10^{-7}–1.0×10^{-2}	59.2
20	6.0×10^{-7}–1.0×10^{-2}	59.4	8.7×10^{-7}–1.0×10^{-2}	59.2
30	2.6×10^{-6}–1.0×10^{-2}	58.5	3.7×10^{-6}–1.0×10^{-2}	58.0
35	5.0×10^{-6}–1.0×10^{-2}	57.9	8.2×10^{-6}–1.0×10^{-2}	57.5
Ethanol				
10	6.0×10^{-7}–1.0×10^{-2}	59.4	8.7×10^{-7}–1.0×10^{-2}	59.2
20	6.0×10^{-7}–1.0×10^{-2}	59.4	8.9×10^{-7}–1.0×10^{-2}	59.1
30	8.5×10^{-6}–1.0×10^{-2}	58.9	2.7×10^{-6}–1.0×10^{-2}	58.4
35	9.2×10^{-6}–1.0×10^{-2}	57.9	7.5×10^{-6}–1.0×10^{-2}	57.6
Acetonitrile				
10	6.0×10^{-7}–1.0×10^{-2}	59.4	8.7×10^{-7}–1.0×10^{-2}	59.2
20	6.1×10^{-7}–1.0×10^{-2}	59.3	8.9×10^{-7}–1.0×10^{-2}	59.1
30	4.5×10^{-6}–1.0×10^{-2}	58.5	4.7×10^{-6}–1.0×10^{-2}	58.3
35	3.1×10^{-6}–1.0×10^{-2}	57.9	5.5×10^{-6}–1.0×10^{-2}	58.0

recommended fixed interference method (FIM) was used to determine the potentiometric selectivity coefficient (SC) for the assumed electrode in the presence of various foreign anions (A^{n-}). The SC in this method was determined using potential measurements of Br^- ion solutions of different concentrations ranging from 10^{-2} to 10^{-8} M and containing a fixed concentration of interfering ions (1.0×10^{-2} M). The SC values for several anions are given in Table 6. Moreover, the SC values for all the interfering ions are less than 1.0; it can be concluded that the proposed Co(II) and Cr(III) complex-based electrodes are highly selective to Br^- ions over the interfering ions studied.[34,35]

The proposed electrodes CoC7 and CrC7 exhibited good performance as indicator electrodes in the potentiometric titration of Br^- ions with $AgNO_3$ and proved their analytical applicability. For this purpose, a 20 mL solution of 1.0×10^{-2} mol L^{-1} NaBr was titrated against 1.0×10^{-1} mol L^{-1} $AgNO_3$ solution at pH 6.0, and the potential response observed using CoC7 and CrC7 are presented in Fig. 7. The resultant titration plot has a conventional sigmoid shape, with a sharp endpoint that matches the 1:1 stoichiometry of the precipitated silver bromide. As a result, potentiometric titration may be used to approximate Br^- ions using the recommended electrodes.

Naturally occurring bromide ions can contaminate drinking water due to excess use of fertilizers and percolation of industrial wastewater in the groundwater. We used the proposed Co(II) complex-based CoC7 and Cr(III) complex-based CrC7 electrodes to assess the Br^- ion concentration in tap water samples. In this study, the tap water samples were initially spiked with Br^- ions at concentrations of 25 mg L^{-1}, 50 mg L^{-1} and 100 mg L^{-1}. Subsequently, 100 mL of every spiked water sample was collected in distinct beakers, and 2 mL of $NaNO_3$ (0.1 M) solution was added as an ionic strength adjuster (ISA). The solution was stirred vigorously before the potentiometric analysis. The results for the estimated Br^- ion concentrations in the tap water samples are

Table 6 Selectivity coefficients of the proposed electrodes for various interfering anions

Interfering anions (B)	Selectivity coefficient ($-\log K_{Br^-, B}$)	
	Electrode CoC7	Electrode CrC7
CN^-	1.38	1.27
SCN^-	1.50	1.31
Sal-	1.84	1.62
F^-	1.43	1.22
NO_2^-	1.62	1.39
Cl^-	1.38	1.18
I^-	1.43	1.17
NO_3^-	1.56	1.26
SO_4^{2-}	2.20	2.30
CO_3^{2-}	1.03	1.05

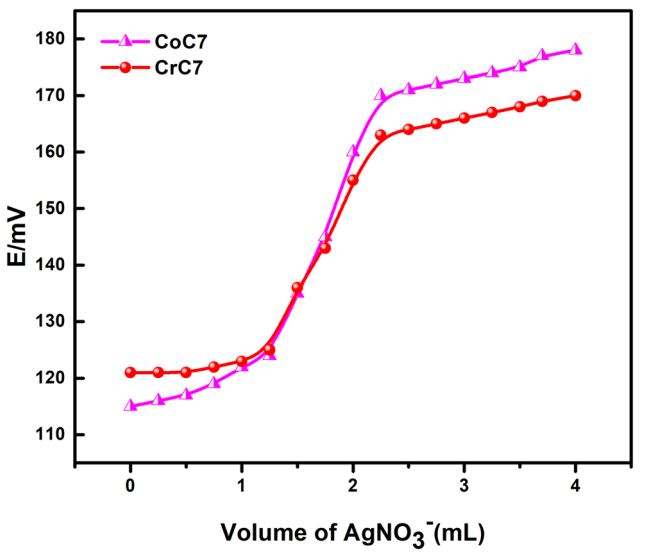

Fig. 7 Potentiometric titration of 20 mL solution of 1.0×10^{-2} mol L^{-1} NaBr against 1.0×10^{-1} mol L^{-1} $AgNO_3$ solution.

Table 7 Potentiometric determination of Br^- ions in tap water samples using the proposed electrodes. Values are presented as mean ± standard deviation of three measurements

Sample no.	Added bromide concentration (mg L^{-1})	Found bromide concentration (mg L^{-1})		
		Sensor CoC7	Sensor CrC7	AAS
1	25	25.3 ± 0.15	25.3 ± 0.12	25.7 ± 0.06
2	50	50.5 ± 0.05	50.4 ± 0.06	50.7 ± 0.12
3	100	101.3 ± 0.05	101.1 ± 0.0.1	101.5 ± 0.06

Table 8 Comparison of the performance of the proposed bromide selective electrodes with the previously reported electrodes

Ref. no	Slope (mV per decade)	Linear range (mol L^{-1})	Detection limit (mol L^{-1})	pH range
15	58.0	10^{-1}–10^{-6}	5.0×10^{-7}	3.5–9.0
16	59.2–60.4	1×10^{-1}–2×10^{-6}	3×10^{-7}	2.0–10.0
17	61 ± 1	1.0×10^{-1}–3.2×10^{-5}	2.0×10^{-5}	4.5–8.5
18	59.1 ± 0.5	10^{-5}–10^{-1}	5.0×10^{-6}	4.0–9.5
19	59.0	7.0×10^{-6}–1.0×10^{-1}	6.0×10^{-6}	3.0–9.0
20	—	1.0×10^{-8}–1.0×10^{-6}	2.0×10^{-9}	—
21	61.0 ± 0.9	3.0×10^{-2}–1.0×10^{-5}	4.0×10^{-6}	4.5–7.5
22	54.53 ± 0.15	1.0×10^{-7}–1.0×10^{-1}	7.1×10^{-8}	—
23	64.4 ± 0.4	1.0×10^{-1}–1.0×10^{-5}	8.0×10^{-6}	6.0–12.0
26	—	1.0×10^{-1}–1.0×10^{-4}	2.2×10^{-5}	4.0–10
24	63 ± 1	1.0×10^{-1}–1.0×10^{-6}	1.6×10^{-5}	2.0–11.0
CoC7	**59.4**	$\mathbf{6.0 \times 10^{-7}}$–$\mathbf{1.0 \times 10^{-2}}$	$\mathbf{5.5 \times 10^{-7}}$	**4.0–9.0**
CrC7	**59.2**	$\mathbf{8.7 \times 10^{-7}}$–$\mathbf{1.0 \times 10^{-2}}$	$\mathbf{6.5 \times 10^{-7}}$	**4.0–9.0**

given in Table 7. The concentrations determined by these electrodes are slightly higher than the amount of Br^- ions added to the test samples, indicating that the bromide ions were already present in tap water samples before the addition. The results of atomic absorption spectrometry (AAS) and potentiometric analysis of the bromide ions in the tap water samples using the proposed electrodes were compared. The results presented in Table 7 demonstrate a significant level of agreement between the two methods, thereby confirming the suggested electrodes' ability for rapid measurement.

The potentiometric characteristics of the developed bromide ion electrodes CoC7 and CrC7 based on Co(II) and Cr(III) salicylidene Schiff base complexes were compared with the previously reported Br^- ion electrodes (Table 8). This comparison revealed that the CoC7 and CrC7 electrodes operate over a wider linear concentration range and exhibit lower detection limits and faster response times than other electrodes. This superior performance is likely due to the strong and durable nature of both complexes, which is important for the longevity and reliability of ion-selective electrodes. In addition, these electrodes exhibited an ideal Nernstian behavior with a very low detection limit, further enhancing their utility and reliability in Br^- ion determination under different environmental conditions.

4. Conclusion

In conclusion, as a new category of bromide ionophores, mononuclear Co(II) and Cr(III) salicylidene Schiff base coordination complexes were synthesized and their potentiometric responses were studied. Both the electrodes demonstrated very high sensitivity with Nernstian slopes of 59.4 ± 0.07 and 59.2 ± 0.04 mV per decade of $[Br^-]$, wide working concentration ranges (6.0×10^{-7}–1.0×10^{-2} mol L^{-1} and 8.7×10^{-7}–1.0×10^{-2} mol L^{-1}) and extremely low detection limits of $5.5 \pm 0.13 \times 10^{-7}$ mol L^{-1} and $6.5 \pm 0.07 \times 10^{-7}$ mol L^{-1}. Operating effectively in the pH range of 4.0 to 9.0, the electrodes exhibited short response times of 12 and 16 seconds and shelf lives of 4 and 5 weeks. A comparative analysis with previously reported sensor setups for bromide detection highlights its superiority over many sensors in terms of detection limit, working concentration range, high selectivity and quick response time. In particular, both cobalt and chromium can exist in multiple oxidation states (*e.g.*, Co(II) and Co(III) and Cr(III) and Cr(IV)), allowing for redox-based sensing mechanisms that may be another reason for this excellent performance. This mechanism is undergoing further investigation, which can be advantageous in designing sensors by switching states upon interconnection with bromide ions to increase the detection capabilities. This work indicates that the transition metal complexes can be considered as a valuable addition to the family of bromide ionophores, promising enhanced accuracy and efficiency in bromide ion detection applications in the areas of food production, pharmaceuticals, and water quality management.

Conflicts of interest

The authors declare no conflict of interest.

Data availability

Supplementary information: The data supporting the findings of this study are available within the article and its SI. The SI includes detailed characterization of the CoC7 and CrC7 complexes, including ATR-FTIR spectroscopy, X-ray diffraction, X-ray photoelectron spectroscopy, and CHN analysis. It also contains Table S1 showing the potentiometric determination of bromide ions in tap water samples using the proposed electrodes. Additional data and materials are available from the corresponding author upon reasonable request. See DOI: **https://doi.org/10.1039/D5SD00088B**.

The original contributions presented in the study are included in the article material; further inquiries can be directed to the corresponding author.

Acknowledgements

We appreciate the financial assistance from the University Grants Commission (UGC), New Delhi, India, to complete this project. This work was supported by the Delaware State through the Center for Advanced Technology seed funding program (Subaward UDR0000546). CHN analytical data were obtained from the CENTC Elemental Analysis Facility at the University of Rochester, funded by NSF CHE-0650456.

References

1 Y. L. Yu, Y. Cai, M. L. Chen and J. H. Wang, Development of a miniature dielectric barrier discharge–optical emission spectrometric system for bromide and bromate screening in environmental water samples, *Anal. Chim. Acta*, 2014, **809**, 30–36, DOI: **10.1016/J.ACA.2013.11.054**.

2 A. García-Figueroa, F. Pena-Pereira, I. Lavilla and C. Bendicho, Headspace single-drop microextraction coupled with microvolume fluorospectrometry for highly sensitive determination of bromide, *Talanta*, 2017, **170**, 9–14, DOI: **10.1016/J.TALANTA.2017.03.090**.

3 J. Marák, A. Staňová, V. Vaváková, M. Hrenáková and D. Kaniansky, On-line capillary isotachophoresis–capillary zone electrophoresis analysis of bromate in drinking waters in an automated analyzer with coupled columns and photometric detection, *J. Chromatogr. A*, 2012, **1267**, 252–258, DOI: **10.1016/J.CHROMA.2012.07.075**.

4 M. Sun, Y. Gao, B. Wei and X. Wu, Determination of iodine and bromine in coal and atmospheric particles by inductively coupled plasma mass spectrometry, *Talanta*, 2010, **81**, 473–476, DOI: **10.1016/J.TALANTA.2009.12.026**.

5 P. Shi, R. Ma, Q. Zhou, A. Li, B. Wu, Y. Miao, X. Chen and X. Zhang, Chemical and bioanalytical assessments on drinking water treatments by quaternized magnetic microspheres, *J. Hazard. Mater.*, 2015, **285**, 53–60, DOI: **10.1016/J.JHAZMAT.2014.09.047**.

6 K. Reddy-Noone, A. Jain and K. K. Verma, Liquid-phase microextraction–gas chromatography–mass spectrometry for the determination of bromate, iodate, bromide and iodide in high-chloride matrix, *J. Chromatogr. A*, 2007, **1148**, 145–151, DOI: **10.1016/J.CHROMA.2007.03.027**.

7 R. D. Rocklin and E. L. Johnson, Determination of Cyanide, Sulfide, Iodide, and Bromide by Ion Chromatography with Electrochemical Detection, *Anal. Chem.*, 1983, **55**, 4–7, DOI: **10.1021/AC00252A005/ASSET/AC00252A005.FP.PNG_V03**.

8 R. W. Keating and P. R. Haddad, Simultaneous determination of ascorbic acid and dehydroascorbic acid by reversed-phase ion-pair high-performance liquid chromatography with pre-column derivatisation, *J. Chromatogr. A*, 1982, **245**, 249–255, DOI: **10.1016/S0021-9673(00)88594-5**.

9 U. Leuenberger, R. Gauch, K. Rieder and E. Baumgartner, Determination of nitrate and bromide in foodstuffs by high-performance liquid chromatography, *J. Chromatogr. A*, 1980, **202**, 461–468, DOI: **10.1016/S0021-9673(00)91832-6**.

10 B. Divjak, M. Novič and W. Goessler, Determination of bromide, bromate and other anions with ion chromatography and an inductively coupled plasma mass spectrometer as element-specific detector, *J. Chromatogr. A*, 1999, **862**, 39–47, DOI: **10.1016/S0021-9673(99)00896-1**.

11 K. Fukushi, K. Watanabe, S. Takeda, S. I. Wakida, M. Yamane, K. Higashi and K. Hiiro, Determination of bromide ions in seawater by capillary zone electrophoresis using diluted artificial seawater as the buffer solution, *J. Chromatogr. A*, 1998, **802**, 211–217, DOI: **10.1016/S0021-9673(97)01218-1**.

12 K. Arai, F. Kusu, N. Noguchi, K. Takamura and H. Osawa, Selective determination of chloride and bromide ions in serum by cyclic voltammetry, *Anal. Biochem.*, 1996, **240**, 109–113, DOI: **10.1006/ABIO.1996.0336**.

13 A. T. Pilipenko, A. V. Terletskaya and O. V. Zui, Determination of iodide and bromide by chemiluminescence methods coupled with dynamic gas extraction, *Z. Anal. Chem.*, 1989, **335**, 45–48, DOI: **10.1007/BF00482390/METRICS**.

14 S. N. Toala, Z. Sun, Y. Yue, S. F. Gonski and W. J. Cai, Recent developments in ionophore-based potentiometric electrochemical sensors for oceanic carbonate detection, *Sens. Diagn.*, 2024, **3**, 599–622, DOI: **10.1039/D3SD00232B**.

15 P. K. C. Tseng and W. F. Gutknecht, The HgS/Hg2Br2-Based Bromide Ion-Selective Electrode, *Anal. Lett.*, 1976, **9**, 795–805, DOI: **10.1080/00032717608059144**.

16 Y. G. Vlasov, L. N. Moskvin, E. A. Bychkov and D. V. Golikov, Silver bromide based chalcogenide glassy-crystalline ion-selective electrodes, *Analyst*, 1989, **114**, 185–190, DOI: **10.1039/AN9891400185**.

17 M. Shamsipur, S. Rouhani, A. Mohajeri, M. R. Ganjali and P. Rashidi-Ranjbar, A bromide ion-selective polymeric membrane electrode based on a benzo-derivative xanthenium bromide salt, *Anal. Chim. Acta*, 2000, **418**, 197–203, DOI: **10.1016/S0003-2670(00)00954-5**.

18 M. R. Ganjali, M. Tahami, T. Poursaberi, A. R. Pazoukian, M. Javanbakht, M. Shamsipur and M. R. Baezat, Novel Bromide Liquid Membrane Electrode, *Anal. Lett.*, 2003, **36**, 347–360, DOI: **10.1081/AL-120017695**.

19 M. R. Ganjali, P. Norouzi, M. Golmohammadi, M. Rezapour and M. Salavati-Niasari, Novel Bromide PVC-Based Membrane Sensor Based on Iron(III)-Salen, *Electroanalysis*, 2004, **16**, 910–914, DOI: **10.1002/ELAN.200302871**.

20 L. Kou and R. Liang, Detection of Bromide Ions in Water Samples with a Nanomolar Detection Limit using a Potentiometric Ion-selective Electrode, *Int. J. Electrochem. Sci.*, 2019, **14**, 1601–1609, DOI: **10.20964/2019.02.02**.

21 M. Shamsipur, S. Ershad, N. Samadi, A. Moghimi and H. Aghabozorg, A novel chemically modified carbon paste electrode based on a new mercury(II) complex for selective potentiometric determination of bromide ion, *J. Solid State Electrochem.*, 2005, **9**, 788–793, DOI: **10.1007/S10008-005-0692-4/TABLES/3**.

22 N. Kaur, J. Kaur, R. Badru, S. Kaushal and P. P. Singh, BGO/AlFu MOF core shell nano-composite based bromide ion-selective electrode, *J. Environ. Chem. Eng.*, 2020, **8**, 104375, DOI: **10.1016/J.JECE.2020.104375**.

23 D. Vlascici, N. Plesu, G. Fagadar-Cosma, A. Lascu, M. Petric, M. Crisan, A. Belean and E. Fagadar-Cosma, Potentiometric Sensors for Iodide and Bromide Based on Pt(II)-Porphyrin, *Sensors*, 2018, **18**, 2297, DOI: **10.3390/S18072297**.

24 A. V. Rzhevskaia, N. V. Shvedene and I. V. Pletnev, Solidified ionic liquid as crystalline sensing element of the bromide selective electrode, *Sens. Actuators, B*, 2014, **193**, 563–567, DOI: **10.1016/J.SNB.2013.11.067**.

25 H. Aghaie, K. Zare, A. R. Abedin and M. Aghaie, Selective Membrane Electrode for Bromide Ion Based on Aza Pyrilium Ion Derivative as a new Ionophore, *Journal of Physical & Theoretical, Chemistry*, 2004, **1**, 27–34, **https://jptc.srbiau.ac.ir/article_6552.html** (accessed June 29, 2024).

26 O. Isildak, O. Özbek and K. M. Yigit, A bromide-selective PVC membrane potentiometric sensor, *Bulg. Chem. Commun.*, 2020, **52**, 448–452, DOI: **10.34049/bcc.52.4.5235**.

27 L. Kafi-Ahmadi and L. Shirmohammadzadeh, Synthesis of Co(II) and Cr(III) salicylidenic Schiff base complexes derived from thiourea as precursors for nano-sized Co3O4 and Cr2O3 and their catalytic, antibacterial properties, *J. Nanostruct. Chem.*, 2017, **7**, 179–190, DOI: **10.1007/S40097-017-0221-X/TABLES/7**.

28 M. C. Biesinger, C. Brown, J. R. Mycroft, R. D. Davidson and N. S. McIntyre, X-ray photoelectron spectroscopy studies of chromium compounds, *Surf. Interface Anal.*, 2004, **36**, 1550–1563, DOI: **10.1002/SIA.1983**.

29 A. A. Memon, A. R. Solangi, S. Memon, A. A. Bhatti and A. A. Bhatti, Highly Selective Determination of Perchlorate by a Calix[4]arene based Polymeric Membrane Electrode, *Polycyclic Aromat. Compd.*, 2016, **36**, 106–119, DOI: **10.1080/10406638.2014.948121**.

30 M. M. Shultz, O. K. Stefanova, S. B. Mokrov and K. N. Mikhelson, Potentiometric estimation of the stability constants of ion-ionophore complexes in ion-selective membranes by the sandwich membrane method: Theory, advantages, and limitations, *Anal. Chem.*, 2002, **74**, 510–517, DOI: **10.1021/AC015564F/ASSET/IMAGES/LARGE/AC015564FF00007.JPEG**.

31 A. Craggs, L. Keil, G. J. Moody and J. D. R. Thomas, An evaluation of solvent mediators for ion-selective electrode membranes based on calcium bis(dialkylphosphate) sensors trapped in poly(vinyl chloride) matrices, *Talanta*, 1975, **22**, 907–910, DOI: **10.1016/0039-9140(75)80191-3**.

32 E. Bakker, P. Bühlmann and E. Pretsch, Carrier-based ion-selective electrodes and bulk optodes. 1. General characteristics, *Chem. Rev.*, 1997, **97**, 3083–3132, DOI: **10.1021/CR940394A/ASSET/IMAGES/MEDIUM/CR940394AE00053.GIF**.

33 U. Schaller, E. Bakker, U. E. Spichiger and E. Pretsch, Ionic Additives for Ion-Selective Electrodes Based on Electrically Charged Carriers, *Anal. Chem.*, 1994, **66**, 391–398, DOI: **10.1021/AC00075A013/ASSET/AC00075A013.FP.PNG_V03**.

34 E. Bakker, E. Pretsch and P. Bühlmann, Selectivity of potentiometric ion sensors, *Anal. Chem.*, 2000, **72**, 1127–1133, DOI: **10.1021/AC991146N/ASSET/IMAGES/LARGE/AC991146NF00006.JPEG**.

35 Y. Umezawa, P. Bühlmann, K. Umezawa, K. Tohda and S. Amemiya, Potentiometric selectivity coefficients of ion-selective electrodes part I. Inorganic cations (technical report), *Pure Appl. Chem.*, 2000, **72**, 1851–2082, DOI: **10.1351/PAC200072101851/MACHINEREADABLECITATION/RIS**.